Published in final edited form as:
Osteoarthritis Cartilage. 2014 September ; 22(9): 1291–1300. doi:10.1016/j.joca.2014.06.035.

Osteochondral Defect Repair Using Bilayered Hydrogels Encapsulating Both Chondrogenically and Osteogenically Pre-differentiated Mesenchymal Stem Cells in a Rabbit Model

Johnny Lam[a], **Steven Lu**[a], **Esther J. Lee**[a], **Jordan E. Trachtenberg**[a], **Ville V. Meretoja**[a], **Rebecca L. Dahlin**[a], **Jeroen J. J. P. van den Beucken**[b], **Yasuhiko Tabata**[c], **Mark E. Wong**[d], **John A. Jansen**[b], **Antonios G. Mikos**[a,*], and **F. Kurtis Kasper**[a,*]

[a]Department of Bioengineering, Rice University, Houston, TX [b]Department of Biomaterials, Radboud umc, Nijmegen, The Netherlands [c]Department of Biomaterials, Institute for Frontier Medical Sciences, Kyoto University, Kyoto, Japan [d]Department of Surgery, Division of Oral and Maxillofacial Surgery, The University of Texas School of Dentistry, Houston, TX

Abstract

Objective—To investigate the ability of cell-laden bilayered hydrogels encapsulating chondrogenically and osteogenically (OS) pre-differentiated mesenchymal stem cells (MSCs) to effect osteochondral defect repair in a rabbit model. By varying the period of chondrogenic pre-differentiation from 7 (CG7) to 14 days (CG14), the effect of chondrogenic differentiation stage on osteochondral tissue repair was also investigated.

Methods—Rabbit MSCs were subjected to either chondrogenic or osteogenic pre-differentiation, encapsulated within respective chondral/subchondral layers of a bilayered hydrogel construct, and then implanted into femoral condyle osteochondral defects. Rabbits were randomized into one of four groups (MSC/MSC, MSC/OS, CG7/OS, and CG14/OS; chondral/subchondral) and received two similar constructs bilaterally. Defects were evaluated after 12 weeks.

*Corresponding Authors: Antonios G. Mikos, Ph.D., Department of Bioengineering, Rice University, P.O. Box 1892, MS-142, Houston, TX 77251-1892, w: 713-348-5355, mikos@rice.edu, F. Kurtis Kasper, Ph.D., Department of Bioengineering, Rice University, P.O. Box 1892, MS-142, Houston, TX 77251-1892, w: 713-348-3027, kasper@rice.edu.

Author Contribution

All authors contributed to either to the conception and design of the study (JL, AGM, FKK), the acquisition, analysis, and interpretation of the data (JL, SL, EJL, JET, VVM, RLD JvdB, JAJ, AGM, FKK), and/or the drafting (JL) and critical revision of the article (JL, SL, VVM, RLD, JvdB, YT, MEW, JAJ, AGM, FKK). All authors approved the final version for submission. JL (johnny.lam@rice.edu), AGM (mikos@rice.edu), and FKK (kasper@rice.edu) assume full responsibility for the integrity of the work outlined in this study.

Competing Interest Statement

All authors report no conflicts of interest as none of the authors received any compensation for this work. The authors also do not hold any financial interests that would cause potential conflicts of interest related to this work.

Results—All groups exhibited similar overall neo-tissue filling. The delivery of OS cells when compared to undifferentiated MSCs in the subchondral construct layer resulted in improvements in neo-cartilage thickness and regularity. However, the addition of CG cells in the chondral layer, with OS cells in the subchondral layer, did not augment tissue repair as influenced by the latter when compared to the control. Instead, CG7/OS implants resulted in more irregular neo- tissue surfaces when compared to MSC/OS implants. Notably, the delivery of CG7 cells, when compared to CG14 cells, with OS cells stimulated morphologically superior cartilage repair. However, neither osteogenic nor chondrogenic pre-differentiation affected detectable changes in subchondral tissue repair.

Conclusions—Cartilage regeneration in osteochondral defects can be enhanced by MSCs that are chondrogenically and osteogenically pre-differentiated prior to implantation. Longer chondrogenic pre-differentiation periods, however, lead to diminished cartilage repair.

Keywords

chondrogenic; osteogenic; pre-differentiation; osteochondral repair; hydrogel; mesenchymal stem cell

1. Introduction

Articular cartilage is a well-studied flexible connective tissue that facilitates the tribological interaction of bones in major diarthrodial joints throughout the body. Despite its seemingly simple structure, the avascular nature of cartilage compromises its endogenous capacity for repair, leading to a high incidence of unresolved cartilage-related injuries [1, 2]. Given the lack of a surgical cure, such cartilage-related injuries still present a substantial economic burden on society [3]. However, significant research advances over the years have allowed for the sophistication of conventional reparative clinical procedures such as marrow stimulation techniques, leading to measurable improvement in patient outcomes [4–7]. Yet, these techniques are contraindicated for larger critical sized lesions, where cell-based regenerative procedures including autologous chondrocyte transplantation (ACT) or matrix-assisted ACT often prove more effective [3, 8]. Nevertheless, modern generation ACT techniques are still unable to obviate significant clinical hurdles involving joint arthrofibrosis, limited donor chondrocyte availability and donor site morbidity.

Articular chondrocytes, being the constituent cell type of native articular cartilage, still represent the standard cell source considered for cell-based cartilage therapies. However, given limited donor supply, mesenchymal stem cells (MSCs) are becoming increasingly coveted as an alternative cell source. Their phenotypic plasticity and renewability make MSCs ideal candidates for the development of new therapies for osteochondral tissue repair. Indeed, the delivery of undifferentiated MSCs to osteochondral defect sites generally confers some therapeutic value [9–16]. However, inconsistencies in efficacy challenge such undirected approaches as viable clinical treatment options [17–20], and suggest that ideal conditions for unlocking the full healing potential of MSCs still remain largely unknown.

Emerging cell-based strategies for osteochondral tissue regeneration are increasingly recognizing the importance of cellular differentiation state and its influence on treatment

outcomes. In particular, it was recently shown that MSCs chondrogenically pre-differentiated with transforming growth factor–β3 (TGF-β3) for 14 days outperformed undifferentiated MSCs and even articular chondrocytes when implanted with a collagen scaffold into an ovine chronic defect model [21]. However, other efforts aiming to leverage the curative properties of chondrogenically pre-differentiated MSCs failed to elicit improved cartilage tissue repair over undifferentiated MSCs [22, 23], indicating that the strategy for pre-differentiation still requires extensive optimization. Toward this effort, our laboratory recently evaluated the chondrogenic and osteogenic capacity of bilayered cell-laden constructs developed using MSCs that have undergone various degrees of pre-differentiation [24]. It was found that MSCs subjected to shorter chondrogenic pre-differentiation periods, when co-cultured with osteogenically pre-differentiated cells, exhibited greater chondrogenic potential as indicated by higher glycosaminoglycan-to-collagen synthetic ratios *in vitro* [24].

Using a similar oligo(poly(ethylene glycol) fumarate) (OPF)-based hydrogel system [25, 26], the present study investigates the ability of these cell-laden constructs to effect osteochondral tissue regeneration *in vivo*. Accordingly, we hypothesized that the delivery of osteogenically pre- differentiated cells in a spatially controlled manner within the subchondral layer of a single bilayered construct would elicit improved histological tissue repair when compared to scaffolds containing only undifferentiated MSCs. It is also hypothesized that the prior chondrogenic pre- differentiation of MSCs encapsulated within the chondral layer with OS cells in the subchondral layer would further enhance osteochondral repair depending on the degree of chondrogenic pre- differentiation. Specifically, the objectives of the study were i.) to measure the effect of osteogenic pre-differentiation of cells in the subchondral layer, ii.) to evaluate the additional effects of chondrogenic pre-differentiation of cells in the chondral layer, and iii.) to assess the influence of chondrogenic pre-differentiation duration of the cells in the chondral layer on key histological markers of osteochondral tissue repair *in vivo* using a rabbit defect model.

2. Materials and Methods

2.1 Experimental Design

As outlined in Table 1, four experimental groups were designed to address the objectives of this study. Briefly, undifferentiated MSCs or MSCs chondrogenically pre-differentiated for 7 (CG7) or 14 days (CG14) were encapsulated with osteogenically pre-differentiated MSCs (OS cells) within respective chondral and subchondral hydrogel layers of the bilayered hydrogel system. The MSC/MSC group was utilized as the experimental control.

2.2 OPF Synthesis and Characterization

OPF macromers were synthesized using poly(ethylene glycol) (PEG) with a nominal molecular weight of 35,000 g/mol (Sigma-Aldrich, St. Louis, MO) following previously established methods [25]. The synthesized OPF was characterized using gel permeation chromatography and stored at −20° C under N_2(g) until use. Prior to use, the polymer was sterilized by ethylene oxide (EO) exposure for 12 hrs following established procedures [27].

2.3 Gelatin Microparticle Fabrication

Gelatin microparticles (GMPs) were fabricated using acidic gelatin of a 5.0 isoelectric point (Nitta Gelatin INC., Osaka, Japan) following well-established methods [28]. Prior to hydrogel encapsulation, sterilized GMPs of 50–100 μm in diameter were swollen in phosphate buffered saline (PBS) (55 μL of PBS per 11 mg of dried GMPs) to achieve swelling according to previously established procedures [29]. GMPs were incorporated into hydrogels to provide moieties for cell-material interactions and to aid hydrogel degradation [30].

2.4 Rabbit Marrow MSC Isolation and Culture

All experimental and surgical protocols for this study were reviewed and approved by the Rice University and The University of Texas Health Science Center Institutional Animal Care and Use Committees (IACUC), and performed according to the National Institutes of Health animal care and use guidelines. Rabbit bone marrow-derived MSCs were harvested from the tibiae of six 6-month old New Zealand white rabbits as previously described [30]. The isolated bone marrow was cultured in general medium (GM) containing low glucose Dulbecco's modified Eagle's medium (LG-DMEM), 10% v/v fetal bovine serum (FBS), and 1% v/v penicillin/streptomycin/fungizone (PSF) for 2 weeks. The rabbit marrow-derived MSCs were then pooled to minimize interanimal variation and cryopreserved until use as previously described [24].

2.5 Pre-differentiation of MSCs

Cryopreserved cells were thawed and expanded in monolayer (3,500 cells/cm^2) in GM before pre-differentiation. The various cell populations used in this study were derived according to a recent study from our laboratory [24]. Accordingly, in order to generate cell populations at varying stages of chondrogenic pre-differentiation, MSCs were first expanded for two weeks and then subjected to either 7 (CG7) or 14 (CG14) days of pre-differentiation in serum-free chondrogenic media containing LG-DMEM, ITS + Premix (6.25 μg/mL insulin, 6.25 μg/mL transferrin, 6.25 μg/mL selenious acid, 5.35 μg/mL linoleic acid, 1.25 μg/mL bovine serum albumin) (BD Biosciences, San Jose, CA), 50 mg/L ascorbic acid, 10^{-7} M dexamethasone, 10 ng/mL TGF-β3 (PeproTech, Rocky Hill, NJ), and 1% v/v PSF. It was shown previously that 7 and 14 days of chondrogenic pre-differentiation using this method led to the production of two phenotypically distinct chondrogenic cell populations [24]. To generate OS cells, MSC cultures were switched after 1 week to complete osteogenic media containing high glucose DMEM, 10% v/v FBS, 50 mg/L ascorbic acid, 10 mM β-glycerophosphate, 10^{-8} M dexamethasone, and 1% v/v PSF 6 days immediately prior to hydrogel encapsulation [31].

2.6 Bilayered Hydrogel Composite Fabrication and MSC Encapsulation

Bilayered hydrogel composites comprising separate subchondral and chondral layers were fabricated from sterile reagents using a two-step crosslinking method [27, 32]. The subchondral layer was first prepared by partially crosslinking the subchondral precursor mixture within a mold, followed by the complete crosslinking of the chondral precursor mixture on top to permit lamination of the two hydrogel layers. Specifically, 100 mg of OPF and 50 mg of poly(ethylene glycol) diacrylate (PEG-DA, M_n 3,400 g/mol; Laysan, Arab, AL) were both

dissolved in 300 μL of PBS and combined with 110 μL of swollen GMP solution. Equal parts (46.8 μL) of the thermal radical initiator solutions, 0.3 M of ammonium persulfate (Sigma Aldrich) and 0.3 M of *N,N,N',N'*–tetramethylethylenediamine (Sigma Aldrich) were then added to the polymer solution to initiate crosslinking. The respective cell suspension (6.7 million cells in 168 μL of PBS) of either MSCs or OS cells was then added in order to obtain a final concentration of 10 million cells per mL. After gentle mixing, the subchondral precursor solution was quickly injected to fill the bottom two-thirds of a cylindrical Teflon mold (2.0 mm in diameter and 2.0 mm in thickness) and incubated at 37° C for 5 min to permit partial crosslinking. Meanwhile, similar precursor solution for the chondral layer was prepared with MSCs or CG cells. The chondral precursor solution was then quickly added on top of the partially crosslinked subchondral hydrogel. The resulting bilayered hydrogel constructs were incubated at 37° C for 10 min to complete the crosslinking reaction. For each animal, bilayered hydrogels were aseptically transferred in serum-free GM and implanted into osteochondral defects within 2 hrs after fabrication. The final dimensions of the cell-laden hydrogel implants after swelling were 3 mm in diameter and 3 mm in height, which match the dimensions of osteochondral defects that were created.

2.7 Animal Surgery

A total of twenty-four skeletally mature, male 6-month old New Zealand White rabbits were utilized in the creation of a full-thickness, bilateral osteochondral defect model based on well-established studies from our laboratory and others [17, 19, 27, 32]. The number of defects, and hence animals used, was determined by power analysis and in consideration of previous *in vivo* studies applying the same model [27, 32]. Anesthesia was induced before surgery by the subcutaneous injection of Ketamine (25-40 mg/kg) and Acepromazine (1-2 mg/kg) and then general anesthesia was maintained via the ventilator administration of a mixture of isoflurane and oxygen.

Critical-sized osteochondral defects (3 mm in diameter and 3 mm in depth) were created in the medial femoral condyles under irrigation using a dental drill. Prefabricated hydrogel implants were then press-fitted into the defect site. Subsequently, the patella was repositioned and the skin and joint capsule were closed. This procedure was repeated for both knees for each animal, with each knee receiving an implant of the same formulation to control for potentially confounding systemic effects. Each animal received two hydrogel implants for a total of 12 repetitions (n=12) for each experimental group.

To minimize discomfort, Carprofen (4 mg/kg) was administered for 3 days postoperatively. All animals were returned to their cages where they were allowed unrestricted weight-bearing activity and were observed for signs of pain, infection, and proper activity.

2.8 Tissue Processing

After 12 weeks, rabbits were euthanized by intravenous administration of Beuthanasia (0.22 mL/kg). Afterward, the tissue surrounding the medial femoral condyle was retrieved *en bloc*. After gross examination, the retrieved specimens were then fixed in 10% neutral buffered formalin for no more than 72 hrs, decalcified in ethylenediaminetetraacetic acid solution for up to 6 weeks, dehydrated through a series of ethanol baths, and embedded in paraffin. 6 μm

thick longitudinal sections were taken from the center (within the central 1 mm), lateral (within the lateral 1 mm), and medial (within the medial 1 mm) edges of each defect using a microtome as previously described [27]. Sections from each defect region were stained with hematoxylin and eosin (H&E), Safranin-O/Fast Green, and van Gieson's Picrofuchsin.

2.9 Histomorphometric Evaluation of Explants

Histological sections from each location of each joint were scored blindly and independently by three evaluators (S.L., V.V.M., and F.K.K.) using a well-established scoring algorithm for osteochondral tissue repair as described previously [27]. 11 total parameters were used to analyze tissue repair for the overall defect as a whole as well as the individual chondral and subchondral regions (Supplemental Table S1). The overall defect repair was evaluated for the percent filling with newly formed tissue and percent degradation of the implant. The chondral defect region was evaluated for repair tissue morphology, thickness, regularity, chondrocyte clustering, and cell/glycosaminoglycan (GAG) content. The cell/GAG content of the cartilage tissue immediately adjacent to the defect was also scored to evaluate any possible degenerative effects from the implant. The subchondral defect region was examined for quality in new tissue filling, integration, and bone morphology.

2.10 Statistical Analysis

The histological scores (mean ± SD) were analyzed using the Wilcoxon Ranked Sum Test with clustering of the data to account for similar bilateral treatments for each animal [33] using SAS JMP Pro v10.0. The effect of implant formulation was also assessed for each knee joint individually between animals using the same statistical analyses. A confidence interval of 95% was utilized and differences were considered significant when $p < 0.05$.

3. Results

3.1 Macroscopic Observations and Gross Tissue Response

All rabbits underwent osteochondral surgery and recovered well. Postoperatively, all twenty-four animals regained mobility within 1 week and resumed normal movement and behavior during the 12-week incubation period. Upon tissue retrieval, no gross signs of swelling, inflammation, or infection were detected on the joint surface for all experimental groups (Supplemental Figure S1a-d).

3.2 Histological Observation

While the morphology of the respective neo-formed bone and cartilage appeared to vary considerably between experimental groups, most samples retained moderate to trace amounts of remaining hydrogel particulates that had not yet fully degraded by 12 weeks (Supplemental Figure S1e).

The newly formed cartilaginous tissue filling the chondral space of osteochondral defects for the MSC/MSC control group was typically thinner than the neighboring native cartilage and retained poor Safranin O staining in half of the observed cases (Figure 1a-c). The newly formed cartilage mainly comprised fibrocartilage at the joint surface and hypertrophic cartilage in the subchondral region (Figure 1d). One of the 12 joints from this group

displayed cortical bone formation in the chondral layer, where a close inspection of the H&E section revealed the presence of osteocytes (Figure 1e).

Neo-cartilage tissue from the MSC/OS group was typically thicker when compared to the adjacent healthy cartilage (Figure 2a-c) and comprised a combination of fibrocartilage and hyaline cartilage with areas of chondrocyte condensation near the osteochondral interface (Figure 2d). Samples from 2 of the 12 MSC/OS joints exhibited high quality articular cartilage regeneration. Many samples also displayed regions of hypertrophy as indicated by both enlarged chondrocytes and differential matrix staining in the chondral defect region (Figure 2e).

The neo-surface tissue morphology of CG14/OS samples ranged considerably from fibrotic to hyaline (Figure 3a-d), with one joint displaying high quality articular cartilage regeneration. At least 10% of samples from the CG14/OS group also resulted in complete disruption of the chondral layer (Figure 3e). In contrast, the neo-surface tissue morphology of CG7/OS samples generally ranged from faintly stained fibrocartilage to more intensely stained hyaline cartilage. Moreover, samples from 2 of the 12 joint defects achieved well-integrated articular cartilage regeneration (Figure 4a-c) with zonal chondrocytic arrangement similar to that of the native tissue (Figure 4d) and displayed no instances of complete surface disruption. New compact and trabecular bone formation can also be seen in the subchondral defect regions of more than 50% of the CG7/OS samples (Figure 4e).

3.3 Histomorphometric Evaluation

The extent of new tissue filling in the overall osteochondral defect and the subchondral region was not different when observed from the center, lateral, or medial locations within the defect (Supplemental Table S2). However, the lateral edge displayed greater neo-cartilage thickness when compared to both the center and medial edge. For joint surface regularity, the medial edge revealed smoother surfaces with fewer fissures when compared to the center and the lateral edge. Lastly, fewer chondrocyte clusters were observed at the medial edge as opposed to the center.

Osteochondral defects from all groups achieved greater than 50% filling with newly formed repair tissue (Table 2). Similar degrees of implant degradation were achieved for all groups, where implants were more than 50% degraded for all samples.

For subchondral tissue repair, changing the cellular constituents of implants did not effect any statistical differences between groups (Table 2). Mean scores for subchondral neo-tissue filling indicated that greater than 50% but less than 100% of the subchondral space was filled with newly formed tissue. The bone morphology score distribution for each group revealed that at least 80% of samples received a score of 1, primarily indicating the presence of fibrous tissue in conjunction with bone (Figure 5a). Despite low morphology scores, the subchondral neo- tissue integrated completely with the surrounding trabecular bone for all formulations as indicated by the mean scores of 3.00 ± 0.00 (Table 2).

For cartilage regeneration, the CG7/OS group resulted in improved neo-cartilage morphology over the CG14/OS group (Table 2). The MSC/OS, CG7/OS, and CG14/OS

groups achieved thicker neo-cartilage repair tissue when compared to the control. Comparing new joint surface regularity, the MSC/OS and CG14/OS groups resulted in neo-cartilage with fewer and smaller fissures when compared to the MSC/MSC group, with MSC/OS samples also scoring higher than CG7/OS samples. For chondrocyte clustering, CG14/OS samples displayed less cluster formation than CG7/OS and MSC/OS samples. Neo-cartilage and adjacent cartilage cell/GAG content remained unaffected. A breakdown of the cartilage histological scores to comparisons between groups within the peripheral edges of each individual knee (left or right), which were more responsive to treatment then the center location (Supplemental Table S3), revealed that the differential responses in neo-cartilage morphology and surface regularity mainly stemmed from the right knee and left knee, respectively (Table 3). Both knees confirmed the differences observed between groups for neo-cartilage thickness. The score distribution for cartilage morphology revealed that only groups containing OS cells in the subchondral layer resulted in articular cartilage regeneration (Figure 5b). Furthermore, CG7/OS implants resulted in the highest percentage of samples exhibiting articular/hyaline cartilage regeneration at 45.7% when compared to other groups.

4. Discussion

The present study demonstrated that the delivery of OS cells via the subchondral layer of the bilayered implants to osteochondral defects led to improvements in neo-cartilage thickness and surface regularity over the control. While addition of CG cells in the chondral layer of the construct did not further influence the degree of cartilage repair, it stimulated a more consistent healing response, where CG7/OS constructs effected the highest percentage of samples with articular or hyaline cartilage regeneration. Remarkably, we found that CG7 cells, when co- delivered with OS cells, stimulated morphologically superior cartilage repair when compared to CG14 cells. However, neither osteogenic nor chondrogenic pre-differentiation affected detectable changes in subchondral tissue repair for this study.

From previous findings, we confirmed that OS cells, when cultured with undifferentiated MSCs in a bilayered hydrogel construct, stimulated the chondrogenic differentiation of the latter likely via paracrine effects [24, 30, 34–36]. In a parallel study, CG cells, when co-cultured with OS cells, displayed enhanced chondrogenic gene expression for type II collagen and aggrecan as well as increased GAG production *in vitro* [24]. Specifically, CG7 cells displayed synthetic profiles with higher GAG-to-collagen ratios when compared to that of CG14 cells in parallel constructs [24] and were more reflective of an immature chondrogenic phenotype [37]. Hence, we hypothesized that chondrogenic and osteogenic pre-differentiation of MSCs prior to their encapsulation within respective chondral and subchondral layers of a bilayered hydrogel construct would improve osteochondral tissue repair upon implantation due to their enhanced but nascent phenotypes.

In the current study, MSC/MSC samples exhibited generally poor cartilage tissue healing, where thin fibrocartilage repair tissues and missing osteochondral interfaces were often observed. Weak Safranin-O staining of newly formed fibrocartilage indicated that undifferentiated MSCs might have stimulated an insufficient healing response by 12 weeks post- implantation. Although research has shown that implanted MSCs can act as powerful

trophic mediators of the host healing response [38] and can augment the chondrogenic matrix production of mature chondrocytes [39], changes to the synovial fluid during injury can alter the cellular transcription of paracrine signaling molecules of MSCs, specifically the up-regulation of pro- inflammatory and angiogenic factors that may complicate healing [40]. This plausibly explains the diminished tissue healing observed from the MSC/MSC group when compared to others.

MSC/OS and CG7/OS samples displaying mainly hyaline or articular cartilage regeneration also commonly displayed regions of chondrogenic foci, or condensations of chondrocytes, near areas involving the repaired osteochondral junction. Such chondrogenic foci formation often indicated growth cartilage that could encourage articular cartilage regeneration and could be modulated by treatment [41, 42]. It is also suggested that chondrogenic foci formation and an aligned osteochondral junction can enable the proper advancement of the subchondral plate during osteochondral tissue repair [42, 43]. Unlike the MSC/MSC samples, CG7/OS and CG14/OS samples did not display instances of bone-like tissue formation in the chondral defect region, suggesting that the implantation of CG and OS cells via a bilayered hydrogel construct allowed the cells to maintain segmentation of the local biochemical environment that is inhibitive toward non-specific phenotypic changes and conducive to composite tissue regeneration. However, increasing the chondrogenic pre-differentiation duration of MSCs from 7 to 14 days prior to their co-delivery with OS cells resulted in an adverse effect on cartilage morphology *in vivo*. While hypertrophy of the CG14 cells was expected to be the cause, CG14 cells from parallel constructs did not actually display any up-regulation of type X collagen gene expression nor adopt hypertrophic changes over 28 days *in vitro* [24]. In a similar study investigating the effect of osteogenic pre-differentiation time on the efficacy of MSCs for bone repair using a rat cranial defect model, it was found that MSCs pre-differentiated for 4 days resulted in the greatest amount of bone formation when compared to 10 and 16 days of pre-differentiation [44]. This effect was attributed to the high proliferation potential of early osteogenic cells and the subsequent increase in synthetic activity of these cells during maturation. The prevalence of less-intensely stained fibrocartilage, resorbing chondrogenic foci [42], and irregular osteochondral junctions observed for the CG14/OS group suggest that the more mature synthetic profile of a lower GAG-to-collagen ratio [24, 35] of CG14 cells may have caused the diminished cartilage repair. Indeed, such results indicate that the degree of successful cartilage repair elicited *in vivo* may not necessarily be directly proportional to the chondrogenic maturation state of the implanted cell-laden cartilage constructs [45].

With regard to subchondral neo-tissue morphology, the range permitted to each score indicated that a score of 1 be given to new tissue comprising any amount of fibrous tissue, including the fibrous encapsulation of remaining hydrogel particulates commonly observed in all groups. Given the relatively short-term *in vivo* implantation period of 12 weeks, the low bone morphology scores may be more an indication of the repair process rather than of chronic tissue scarring. Hence, samples that displayed fibrous encapsulation consistent with a normal healing response, which eventually remodels into trabecular bone [46], were also included in this score. The presence of particulates only in the subchondral region, in addition to the improved cartilage scores at the peripheral edges as compared to the center,

suggest that repair began from the periphery and migrated inward [47]. Moreover, increased shear and compressive forces during ambulation may have caused faster degradation of the implant near the joint surface, allowing the growth of peripheral repair tissue closing the defect surface to push the remaining implant material downwards into the slower growing subchondral defect region.

While the current scoring algorithm allows for assessment of the individual chondral and subchondral tissues as well as the whole defect [32, 48], it may overlook smaller but potentially significant changes in extracellular matrix structure and tissue response. Indeed, the impact of the present study would be greatly improved with the inclusion of more refined microscopic methodologies including *in vivo* biochemical and gene expression analyses, immunohistochemistry for specific extracellular matrix markers, quantitative polarized light microscopy [49] for assessment of cartilage structure and micro-computed tomography [50] for assessment of bone mineralization. However, such techniques are still experimental and do not yet represent standard assessment tools for *in vivo* osteochondral defect repair. Another weakness of the study was the lack of cell tracking in order to elucidate cell fate after implantation. Cell tracking was not employed in the present study given its unclear effects on the nature of the cellular pre-differentiation scheme used. Lastly, a larger animal model and a longer implantation period would be necessary in order to fully assess robust tissue repair.

In summary, we show that the therapeutic efficacy of MSCs on cartilage regeneration in osteochondral tissue defects can be enhanced by chondrogenic and osteogenic pre-differentiation prior to implantation. Additionally, differences in morphological outcomes as affected by changes to the chondrogenic pre-differentiation duration reveal that cell phenotype could be optimized in order to achieve ideal tissue repair. Furthermore, we present a unique method for the delivery of multiple cell types in order to achieve local biochemical environments conducive to tissue regeneration while mitigating the non-specific and dosage limitations of growth factor therapies.

Supplementary Material

Refer to Web version on PubMed Central for supplementary material.

Acknowledgments

We especially thank Natasja van Dijk for her technical expertise with tissue histology. We would also like to thank the registered veterinary technicians at the University of Texas Health Science Center for their support during the animal procedures.

Role of Funding Source

This work was supported by the National Institutes of Health (R01 AR048756). The study sponsors had no involvement in the study design nor the collection, analysis, interpretation of data. The study sponsors also had no involvement in neither the writing of the manuscript nor the decision to submit the manuscript for publication.

References

1. Cheng YJ, Hootman JM, Murphy LB, Langmaid GA, Helmick CG. Prevalence of doctor- diagnosed arthritis and arthritis-attributable activity limitation - United States: 2007 – 2009. Morbidity and Mortality Weekly Report. 2010; 59:1261–1265. [PubMed: 20930703]
2. Widuchowski W, Widuchowski J, Trzaska T. Articular cartilage defects: study of 25,124 knee arthroscopies. Knee. 2007; 14:177–182. [PubMed: 17428666]
3. Behery O, Siston RA, Harris JD, Flanigan DC. Treatment of cartilage defects of the knee: expanding on the existing algorithm. Clin J Sport Med. 2014; 24:21–30. [PubMed: 24157464]
4. Buschmann, MD.; Hoemann, CD.; Hurtig, MB.; Shive, MS. Cartilage Repair Strategies Totowa. New Jersey: Humana Press; 2007. Cartilage Repair with Chitosan- Glycerol Phosphate-Stabilized Blood Clots; p. 85-104.
5. Gille J, Schuseil E, Wimmer J, Gellissen J, Schulz AP, Behrens P. Mid-term results of Autologous Matrix-Induced Chondrogenesis for treatment of focal cartilage defects in the knee. Knee Surg Sports Traumatol Arthrosc. 2010; 18:1456–1464. [PubMed: 20127072]
6. Kuo AC, Rodrigo JJ, Reddi AH, Curtiss S, Grotkopp E, Chiu M. Microfracture and bone morphogenetic protein 7 (BMP-7) synergistically stimulate articular cartilage repair. Osteoarthritis Cartilage. 2006; 14:1126–1135. [PubMed: 16765606]
7. Mithoefer K. Complex articular cartilage restoration. Sports Med Arthrosc. 2013; 21:31–37. [PubMed: 23314266]
8. Micheli LJ, Browne JE, Erggelet C, Fu F, Mandelbaum B, Moseley JB, et al. Autologous chondrocyte implantation of the knee: multicenter experience and minimum 3-year follow-up. Clin J Sport Med. 2001; 11:223–228. [PubMed: 11753058]
9. Hennig T, Lorenz H, Thiel A, Goetzke K, Dickhut A, Geiger F, et al. Reduced chondrogenic potential of adipose tissue derived stromal cells correlates with an altered TGFbeta receptor and BMP profile and is overcome by BMP-6. J Cell Physiol. 2007; 211:682–691. [PubMed: 17238135]
10. Im GI, Kim DY, Shin JH, Hyun CW, Cho WH. Repair of cartilage defect in the rabbit with cultured mesenchymal stem cells from bone marrow. J Bone Joint Surg Br. 2001; 83:289–294. [PubMed: 11284583]
11. Qi Y, Zhao T, Xu K, Dai T, Yan W. The restoration of full-thickness cartilage defects with mesenchymal stem cells (MSCs) loaded and cross-linked bilayer collagen scaffolds on rabbit model. Mol Biol Rep. 2012; 39:1231–1237. [PubMed: 21594730]
12. Shirasawa S, Sekiya I, Sakaguchi Y, Yagishita K, Ichinose S, Muneta T. In vitro chondrogenesis of human synovium-derived mesenchymal stem cells: optimal condition and comparison with bone marrow-derived cells. J Cell Biochem. 2006; 97:84–97. [PubMed: 16088956]
13. Tay LX, Ahmad RE, Dashtdar H, Tay KW, Masjuddin T, Ab-Rahim S, et al. Treatment outcomes of alginate-embedded allogenic mesenchymal stem cells versus autologous chondrocytes for the repair of focal articular cartilage defects in a rabbit model. Am J Sports Med. 2012; 40:83–90. [PubMed: 21917609]
14. Wakitani S, Goto T, Pineda SJ, Young RG, Mansour JM, Caplan AI, et al. Mesenchymal cell-based repair of large, full-thickness defects of articular cartilage. J Bone Joint Surg Am. 1994; 76:579–592. [PubMed: 8150826]
15. Wang Y, Kim UJ, Blasioli DJ, Kim HJ, Kaplan DL. In vitro cartilage tissue engineering with 3D porous aqueous-derived silk scaffolds and mesenchymal stem cells. Biomaterials. 2005; 26:7082–7094. [PubMed: 15985292]
16. Yan H, Yu C. Repair of full-thickness cartilage defects with cells of different origin in a rabbit model. Arthroscopy. 2007; 23:178–187. [PubMed: 17276226]
17. Anderson JA, Little D, Toth AP, Moorman CT 3rd, Tucker BS, Ciccotti MG, et al. Stem Cell Therapies for Knee Cartilage Repair: The Current Status of Preclinical and Clinical Studies. Am J Sports Med. 2013
18. Chang CH, Kuo TF, Lin FH, Wang JH, Hsu YM, Huang HT, et al. Tissue engineering- based cartilage repair with mesenchymal stem cells in a porcine model. J Orthop Res. 2011; 29:1874–1880. [PubMed: 21630328]

19. Guo X, Park H, Young S, Kretlow JD, van den Beucken JJ, Baggett LS, et al. Repair of osteochondral defects with biodegradable hydrogel composites encapsulating marrow mesenchymal stem cells in a rabbit model. Acta Biomater. 2010; 6:39–47. [PubMed: 19660580]
20. Tang QO, Carasco CF, Gamie Z, Korres N, Mantalaris A, Tsiridis E. Preclinical and clinical data for the use of mesenchymal stem cells in articular cartilage tissue engineering. Expert Opin Biol Ther. 2012; 12:1361–1382. [PubMed: 22784026]
21. Zscharnack M, Hepp P, Richter R, Aigner T, Schulz R, Somerson J, et al. Repair of chronic osteochondral defects using predifferentiated mesenchymal stem cells in an ovine model. Am J Sports Med. 2010; 38:1857–1869. [PubMed: 20508078]
22. Dashtdar H, Rothan HA, Tay T, Ahmad RE, Ali R, Tay LX, et al. A preliminary study comparing the use of allogenic chondrogenic pre-differentiated and undifferentiated mesenchymal stem cells for the repair of full thickness articular cartilage defects in rabbits. J Orthop Res. 2011; 29:1336–1342. [PubMed: 21445989]
23. Grayson WL, Bhumiratana S, Grace Chao PH, Hung CT, Vunjak-Novakovic G. Spatial regulation of human mesenchymal stem cell differentiation in engineered osteochondral constructs: effects of pre-differentiation, soluble factors and medium perfusion. Osteoarthritis Cartilage. 2010; 18:714–723. [PubMed: 20175974]
24. Lam J, Lu S, Meretoja VV, Tabata Y, Mikos AG, Kasper FK. Generation of osteochondral tissue constructs with chondrogenically and osteogenically predifferentiated mesenchymal stem cells encapsulated in bilayered hydrogels. Acta Biomater. 2013
25. Kinard LA, Kasper FK, Mikos AG. Synthesis of oligo(poly(ethylene glycol) fumarate). Nat Protoc. 2012; 7:1219–1227. [PubMed: 22653160]
26. Lam J, Kim K, Lu S, Tabata Y, Scott DW, Mikos AG, et al. A factorial analysis of the combined effects of hydrogel fabrication parameters on the in vitro swelling and degradation of oligo(poly(ethylene glycol) fumarate) hydrogels. J Biomed Mater Res A. 2013
27. Kim K, Lam J, Lu S, Spicer PP, Lueckgen A, Tabata Y, et al. Osteochondral tissue regeneration using a bilayered composite hydrogel with modulating dual growth factor release kinetics in a rabbit model. J Control Release. 2013; 168:166–178. [PubMed: 23541928]
28. Holland TA, Tabata Y, Mikos AG. In vitro release of transforming growth factor-beta 1 from gelatin microparticles encapsulated in biodegradable, injectable oligo(poly(ethylene glycol) fumarate) hydrogels. J Control Release. 2003; 91:299–313. [PubMed: 12932709]
29. Holland TA, Tessmar JK, Tabata Y, Mikos AG. Transforming growth factor-beta 1 release from oligo(poly(ethylene glycol) fumarate) hydrogels in conditions that model the cartilage wound healing environment. J Control Release. 2004; 94:101–114. [PubMed: 14684275]
30. Guo X, Liao J, Park H, Saraf A, Raphael RM, Tabata Y, et al. Effects of TGF-beta3 and preculture period of osteogenic cells on the chondrogenic differentiation of rabbit marrow mesenchymal stem cells encapsulated in a bilayered hydrogel composite. Acta Biomater. 2010; 6:2920–2931. [PubMed: 20197126]
31. Guo X, Park H, Liu G, Liu W, Cao Y, Tabata Y, et al. In vitro generation of an osteochondral construct using injectable hydrogel composites encapsulating rabbit marrow mesenchymal stem cells. Biomaterials. 2009; 30:2741–2752. [PubMed: 19232711]
32. Holland TA, Bodde EW, Cuijpers VM, Baggett LS, Tabata Y, Mikos AG, et al. Degradable hydrogel scaffolds for in vivo delivery of single and dual growth factors in cartilage repair. Osteoarthritis Cartilage. 2007; 15:187–197. [PubMed: 16965923]
33. Bryant D, Havey TC, Roberts R, Guyatt G. How many patients? How many limbs? Analysis of patients or limbs in the orthopaedic literature: Asystematic review. Journal of Bone and Joint Surgery-American Volume. 2006; 88A:41–45.
34. Rothenberg AR, Ouyang L, Elisseeff JH. Mesenchymal stem cell stimulation of tissue growth depends on differentiation state. Stem Cells Dev. 2011; 20:405–414. [PubMed: 20887213]
35. Chen WH, Lai MT, Wu AT, Wu CC, Gelovani JG, Lin CT, et al. In vitro stage-specific chondrogenesis of mesenchymal stem cells committed to chondrocytes. Arthritis Rheum. 2009; 60:450–459. [PubMed: 19180515]

36. Thibault RA, Mikos AG, Kasper FK. Protein and mineral composition of osteogenic extracellular matrix constructs generated with a flow perfusion bioreactor. Biomacromolecules. 2011; 12:4204–4212. [PubMed: 22040097]
37. Williamson AK, Chen AC, Sah RL. Compressive properties and function-composition relationships of developing bovine articular cartilage. J Orthop Res. 2001; 19:1113–1121. [PubMed: 11781013]
38. Caplan AI, Dennis JE. Mesenchymal stem cells as trophic mediators. J Cell Biochem. 2006; 98:1076–1084. [PubMed: 16619257]
39. Wu L, Leijten JC, Georgi N, Post JN, van Blitterswijk CA, Karperien M. Trophic effects of mesenchymal stem cells increase chondrocyte proliferation and matrix formation. Tissue Eng Part A. 2011; 17:1425–1436. [PubMed: 21247341]
40. Vezina Audette R, Lavoie-Lamoureux A, Lavoie JP, Laverty S. Inflammatory stimuli differentially modulate the transcription of paracrine signaling molecules of equine bone marrow multipotent mesenchymal stromal cells. Osteoarthritis Cartilage. 2013; 21:1116–1124. [PubMed: 23685224]
41. Chen H, Chevrier A, Hoemann CD, Sun J, Lascau-Coman V, Buschmann MD. Bone marrow stimulation induces greater chondrogenesis in trochlear vs condylar cartilage defects in skeletally mature rabbits. Osteoarthritis Cartilage. 2013; 21:999–1007. [PubMed: 23611900]
42. Chevrier A, Hoemann CD, Sun J, Buschmann MD. Temporal and spatial modulation of chondrogenic foci in subchondral microdrill holes by chitosan-glycerol phosphate/blood implants. Osteoarthritis Cartilage. 2011; 19:136–144. [PubMed: 21044693]
43. Qiu YS, Shahgaldi BF, Revell WJ, Heatley FW. Observations of subchondral plate advancement during osteochondral repair: a histomorphometric and mechanical study in the rabbit femoral condyle. Osteoarthritis Cartilage. 2003; 11:810–820. [PubMed: 14609534]
44. Castano-Izquierdo H, Alvarez-Barreto J, van den Dolder J, Jansen JA, Mikos AG, Sikavitsas VI. Pre-culture period of mesenchymal stem cells in osteogenic media influences their in vivo bone forming potential. J Biomed Mater Res A. 2007; 82:129–138. [PubMed: 17269144]
45. Fisher MB, Henning EA, Soegaard NB, Dodge GR, Steinberg DR, Mauck RL. Maximizing cartilage formation and integration via a trajectory-based tissue engineering approach. Biomaterials. 2014; 35:2140–2148. [PubMed: 24314553]
46. Holland TA, Bodde EWH, Baggett LS, Tabata Y, Mikos AG, Jansen JA. Osteochondral repair in the rabbit model utilizing bilayered, degradable oligo(poly(ethylene glycol) fumarate) hydrogel scaffolds. Journal of Biomedical Materials Research Part A. 2005; 75A:156–167. [PubMed: 16052490]
47. Brun P, Dickinson SC, Zavan B, Cortivo R, Hollander AP, Abatangelo G. Characteristics of repair tissue in second-look and third-look biopsies from patients treated with engineered cartilage: relationship to symptomatology and time after implantation. Arthritis Res Ther. 2008; 10:R132. [PubMed: 19014452]
48. Orth P, Zurakowski D, Wincheringer D, Madry H. Reliability, reproducibility, and validation of five major histological scoring systems for experimental articular cartilage repair in the rabbit model. Tissue Eng Part C Methods. 2012; 18:329–339. [PubMed: 22081995]
49. Raub CB, Hsu SC, Chan EF, Shirazi R, Chen AC, Chnari E, et al. Microstructural remodeling of articular cartilage following defect repair by osteochondral autograft transfer. Osteoarthritis Cartilage. 2013; 21:860–868. [PubMed: 23528954]
50. Chang NJ, Lam CF, Lin CC, Chen WL, Li CF, Lin YT, et al. Transplantation of autologous endothelial progenitor cells in porous PLGA scaffolds create a microenvironment for the regeneration of hyaline cartilage in rabbits. Osteoarthritis Cartilage. 2013; 21:1613–1622. [PubMed: 23927932]

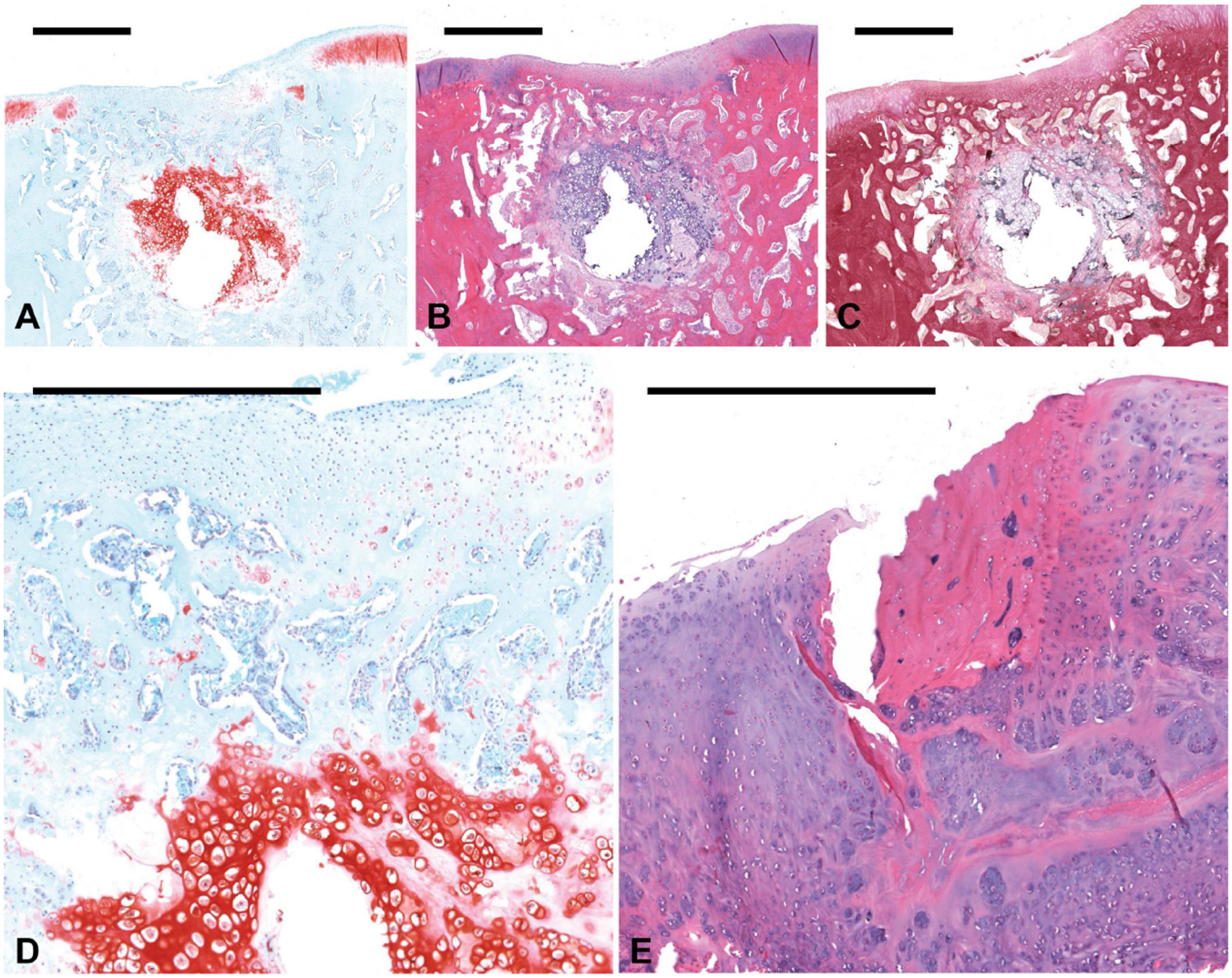

Figure 1.

Histological sections showing representative osteochondral tissue repair at 12 weeks postoperatively for the MSC/MSC group. Sections were stained with (a) Safranin O/Fast Green, (b) H&E, and (c) van Gieson's Picrofuchsin (scale bars: 1000 μm). Images from this sample (a- c), which received a score of 2 for cartilage morphology, showed thin fibrocartilage formation filling the chondral defect space and ossifying chondrocytes in the subchondral defect space. (d) The newly formed cartilage in the osteochondral defect mostly comprised fibrocartilage at the joint surface and hypertrophic cartilage in the subchondral region (scale bar: 500 μm). (e) One other joint from the MSC/MSC group displayed bone-like tissue formation in the chondral defect region, as can be seen by the presence of osteocytes in the H&E section (scale bar: 500 μm).

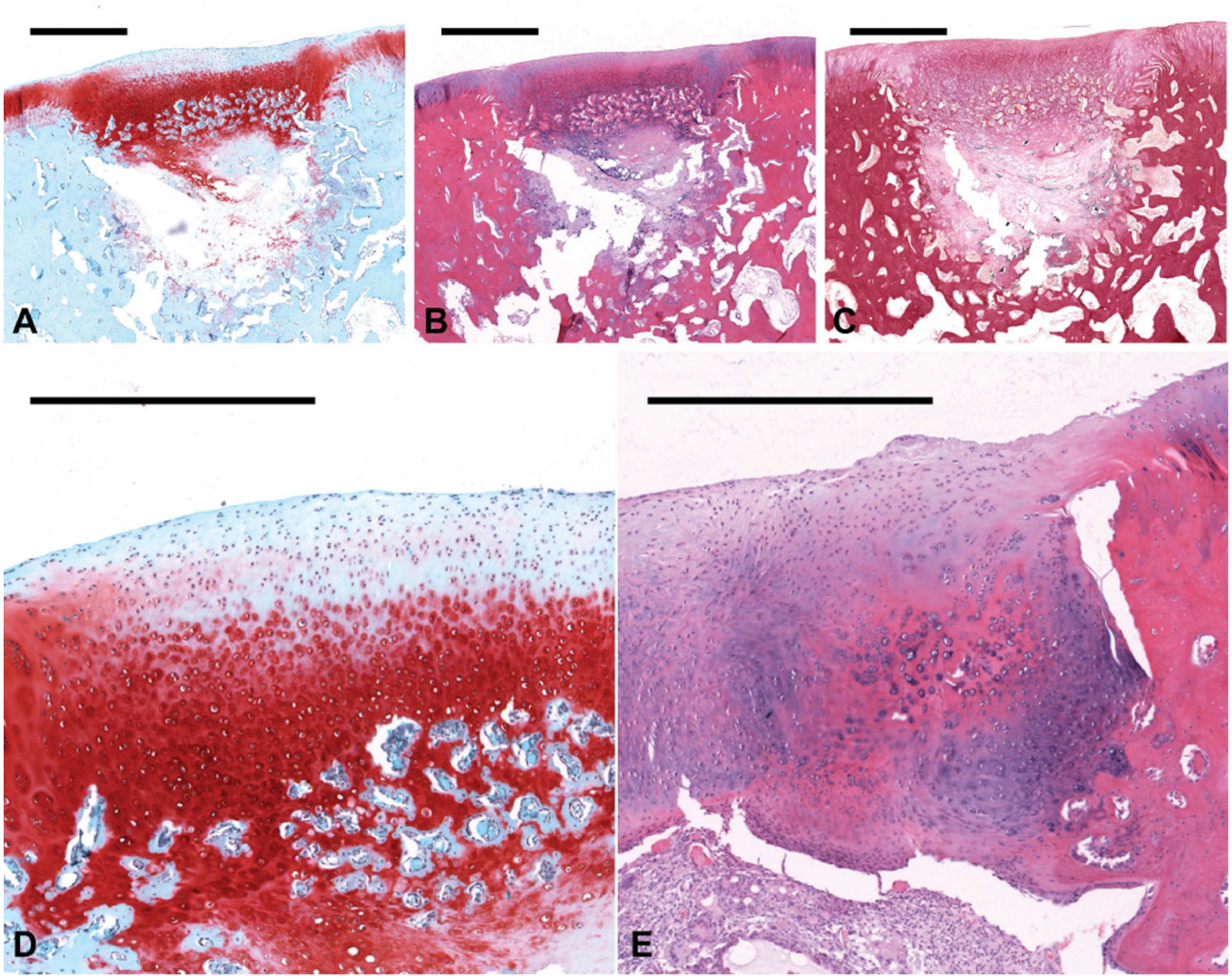

Figure 2.

Histological sections showing representative osteochondral tissue repair at 12 weeks postoperatively for the MSC/OS group. Sections were stained with (a) Safranin O/Fast Green, (b) H&E, and (c) van Gieson's Picrofuchsin (scale bars: 1000 μm). (d) This sample, which received a score of 2 for cartilage morphology, displayed thicker cartilage formation, which mainly comprised a mixture of fibro- and hyaline cartilage (scale bar: 500 μm). This sample also showed the development of a relatively discernable osteochondral interface. (e) An example of regional hypertrophy in the chondral portion of the defect from another sample displayed enlarged chondrocytes and differential matrix staining when compared to the surrounding cartilage (scale bar: 500 μm).

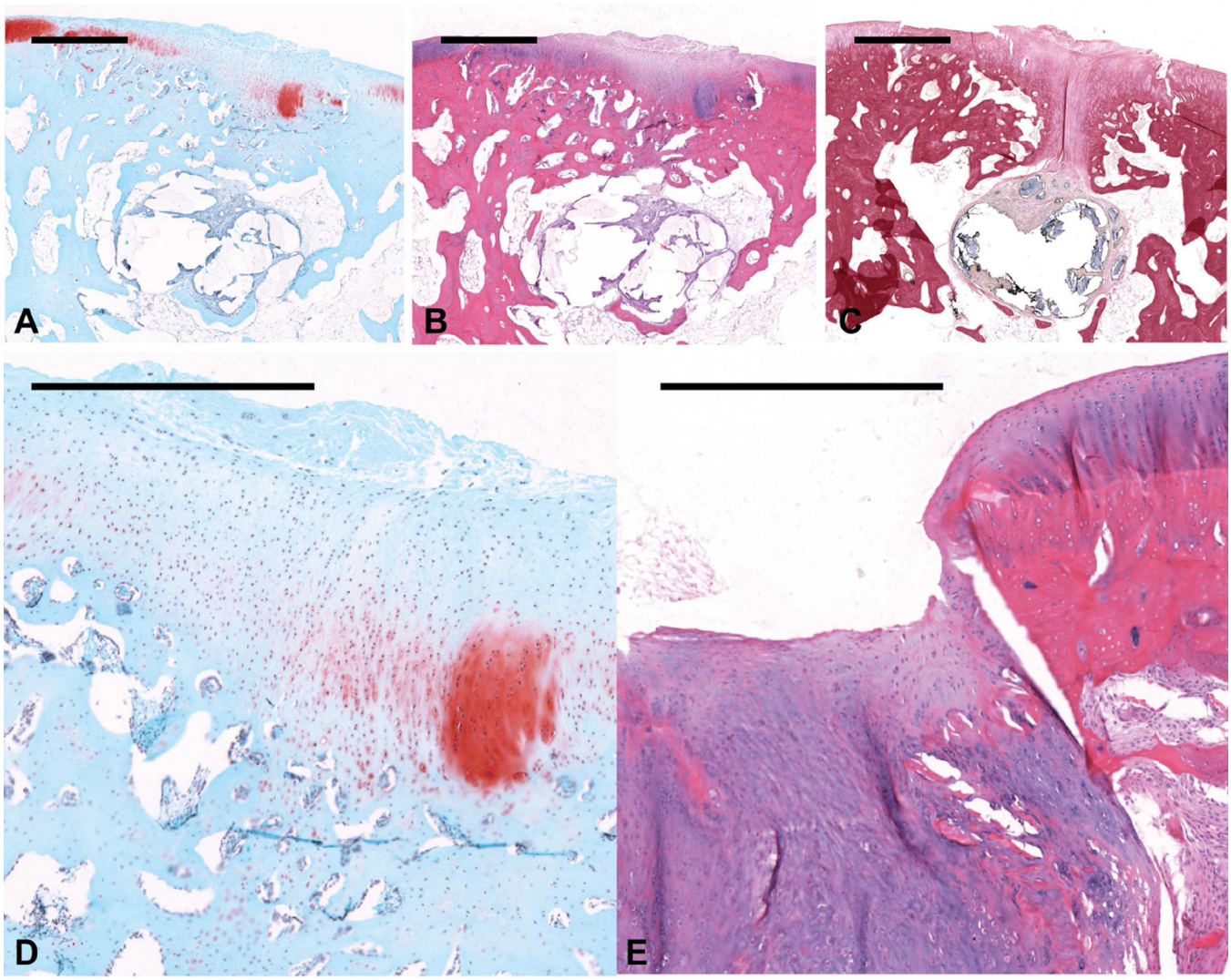

Figure 3.

Histological sections showing representative osteochondral tissue repair at 12 weeks postoperatively for the CG14/OS group. Sections were stained with (a) Safranin O/Fast Green, (b and d) H&E, and (c) van Gieson's Picrofuchsin (scale bars: 1000 μm). (d) This sample , which received a score of 2 for cartilage morphology, showed primarily fibrocartilage tissue repair with some fibrous tissue formation at the joint surface (scale bar: 500 μm). (e) One example of joint surface disruption in another sample is shown in the H&E section (scale bar: 500 μm).

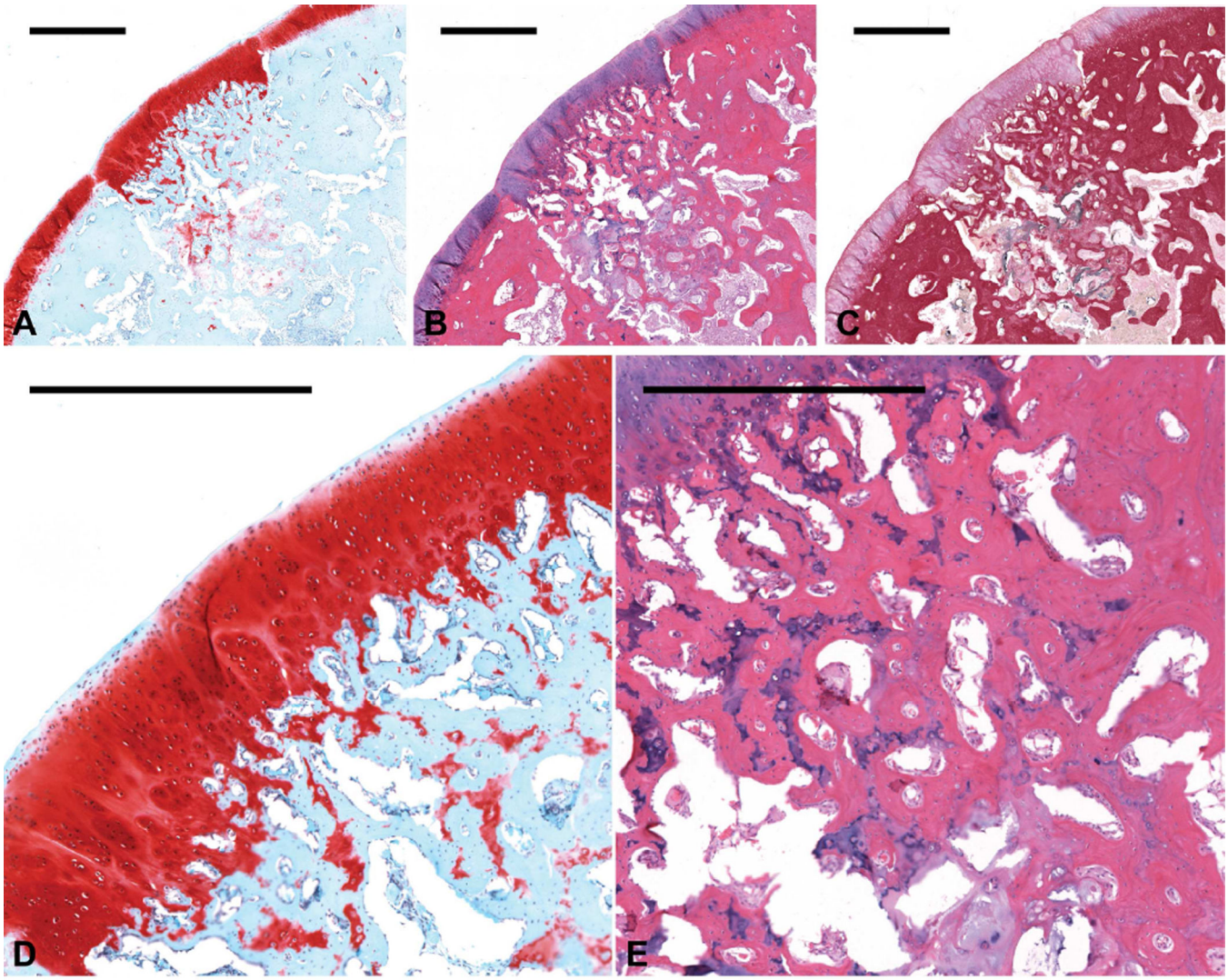

Figure 4.

Histological sections showing representative osteochondral tissue repair at 12 weeks postoperatively for the CG7/OS group. Sections were stained with (a) Safranin O/Fast Green, (b) H&E, and (c) van Gieson's Picrofuchsin (scale bars: 1000 μm). (d) This sample, which received a score of 4 for cartilage morphology, displayed high quality articular cartilage with columnar arrangement of chondrocytes (scale bars: 1000 μm). (e) This sample also displayed compact and trabecular bone formation in the subchondral defect regions of the osteochondral defects (scale bars: 1000 μm).

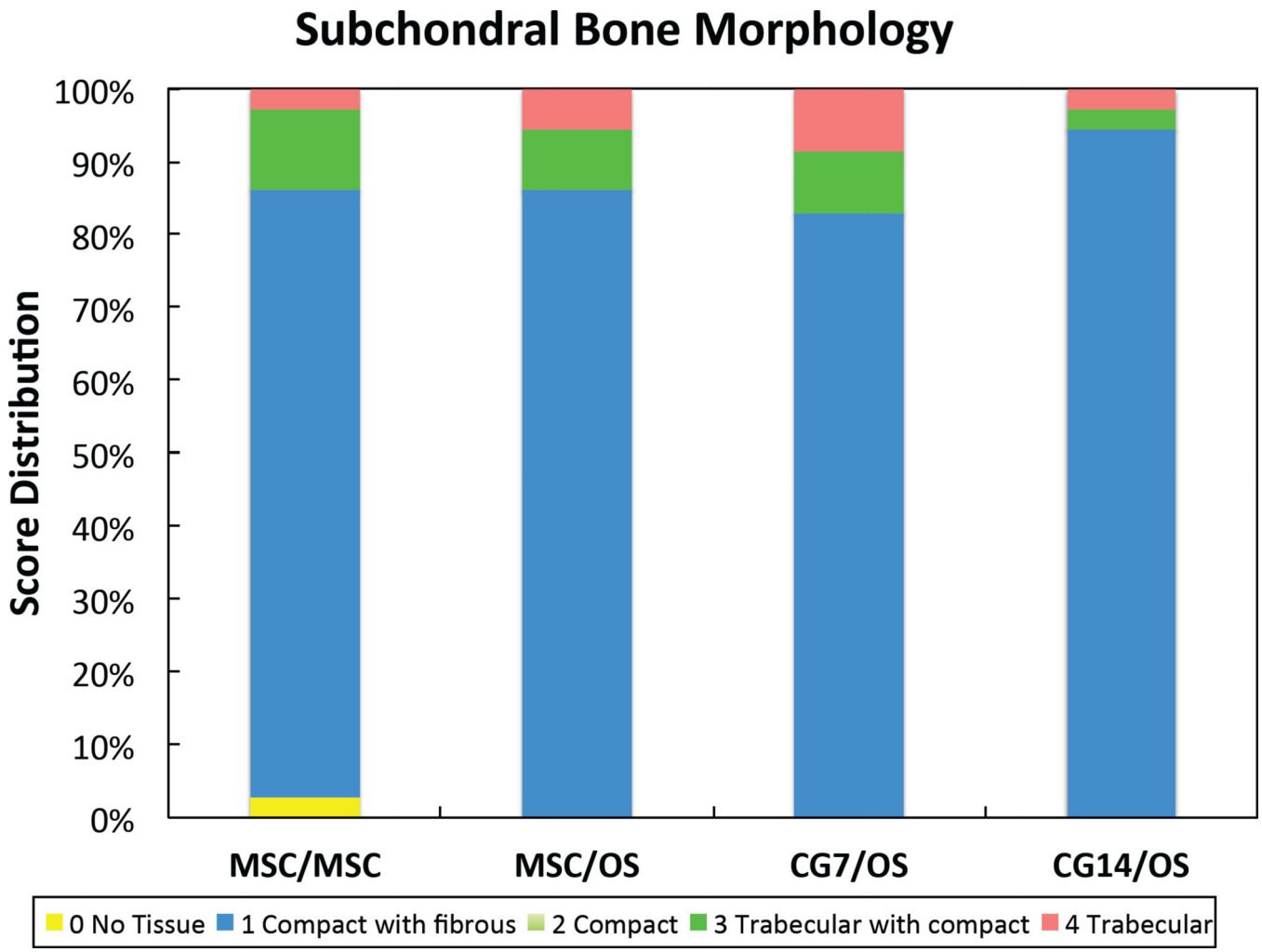

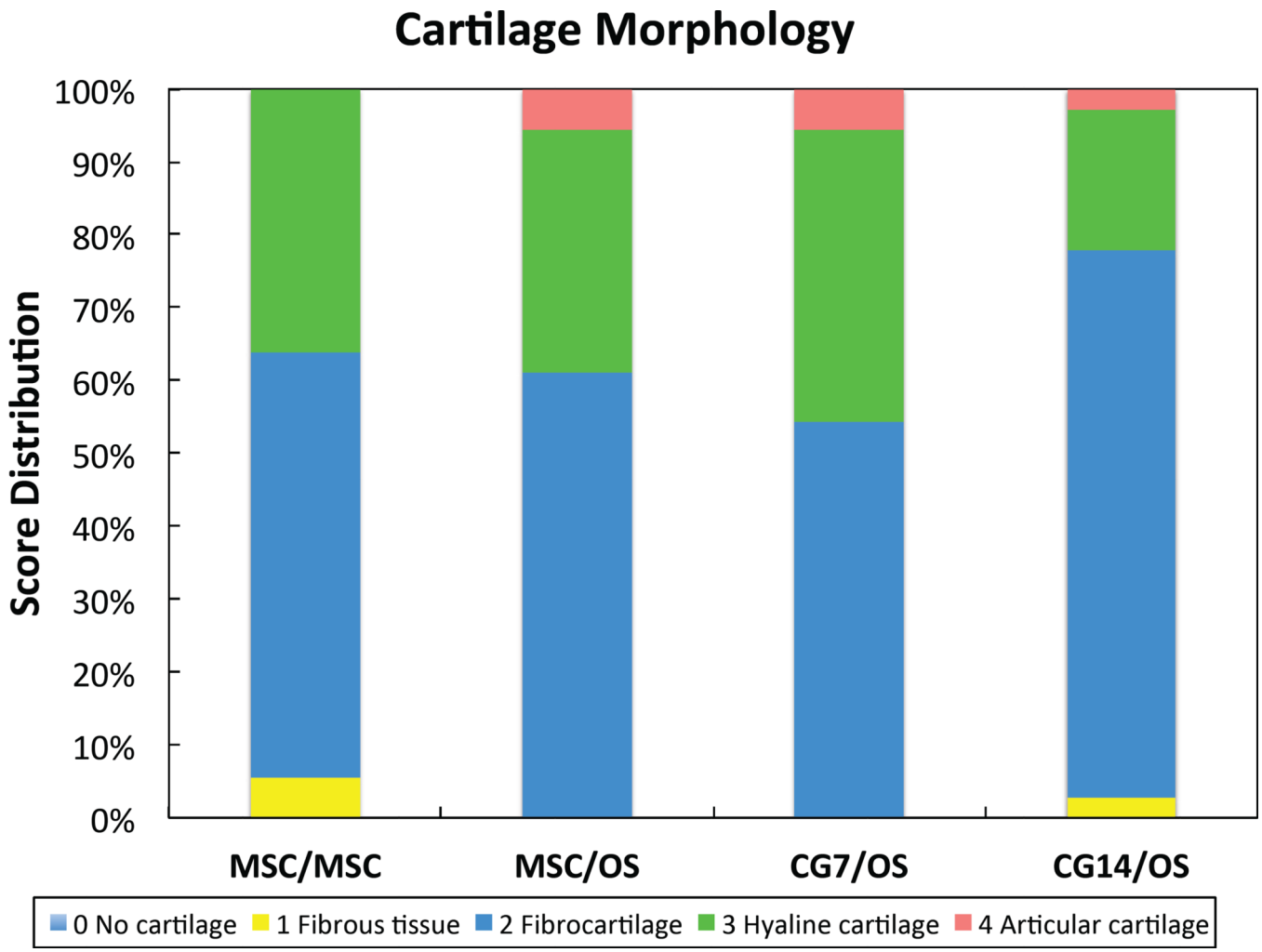

Figure 5.
Histological score distribution for the new (a) subchondral bone morphology and the new (b) cartilage tissue morphology.

Table 1

Cell-laden bilayered hydrogel design for the four formulations evaluated in this study. For each group, 6 animals were used.

Experimental Groups			MSC/MSC (12 implants)	MSC/OS (12 implants)	CG7/OS (12 implants)	CG14/OS (12 implants)
OPF Hydrogel Precursor Solution						
Cartilage Layer (Top 1 mm)	10 mM GMPs	mg per 100 mg OPF	22	22	22	22
	Cell Suspension	Cell Population	MSC	MSC	CG7	CG14
		CG Pre-differentiation Duration (Before Encapsulation)	0 Days	0 Days	7 Days	14 Days
		Encapsulation Density (million per mL precursor)	10	10	10	10
Subchondral Layer (Bottom 2 mm)	10 mM GMPs	mg per 100 mg OPF	22	22	22	22
	Cell Suspension	Cell Population	MSC	OS	OS	OS
		OS Pre-differentiation Duration (Before Encapsulation)	0 Days	6 Days	6 Days	6 Days
		Encapsulation Density (million per mL precursor)	10	10	10	10
Description			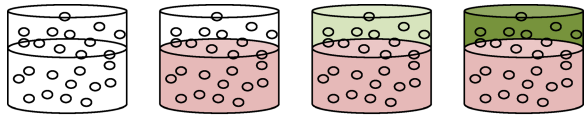 Black Circles: GMPs White: Undifferentiated MSCs Pink: Osteogenic Cells Light Green: Chondrogenic Cells (7 days) Dark Green: Chondrogenic Cells (14 days)			

Table 2

Mean histological scores for all hydrogel formulations at the center, lateral edge, and medial edge of the defect 12 weeks postsurgery.

	Mean Overall Scores			
Histological Paramter	**MSC/MSC (12 knees)**	**MSC/OS (12 knees)**	**CG7/OS (12 knees)**	**CG14/OS (12 knees)**
Overall defect evaluation				
1. Percent filling with newly formed tissue	2.2±0.4	2.2±0.4	2.1±0.5	2.1±0.3
2. Percent degradation of the implant	2.2±0.4	2.2±0.4	2.2±0.5	2.1±0.3
Subchondral bone evaluation				
3. Percent filling with newly formed tissue	2.2±0.5	2.1±0.5	2.1±0.6	2.0±0.3
4. Subchondral bone morphology	1.3±0.8	1.3±0.9	1.5±1.0	1.1±0.6
5. Extent of new tissue bonding with adjacent bone	3.0±0.0	3.0±0.0	3.0±0.0	3.0±0.0
Cartilage evaluation				
6. Morphology of newly formed surface tissue	2.3±0.6	2.4±0.6	2.5±0.6[d]	2.2±0.5[c]
7. Thickness of newly formed cartilage	1.5±0.7[b,c,d]	2.1±0.6[a]	1.9±0.8[a]	1.9±0.6[a]
8. Joint surface regularity	1.9±0.9[b,d]	2.4±0.8[a,c]	2.2±0.6[b]	2.3±1.0[a]
9. Chondrocyte clustering	2.1±0.5	2.0±0.3[d]	2.1±0.4[d]	2.3±0.5[b,c]
10. Chondrocyte and GAG content of neocartilage	1.8±0.8	1.9±0.7	1.9±0.7	1.8±0.7
11. Chondrocyte and GAG content, of adjacent cartilage	2.8±0.4	2.6±0.6	2.8±0.5	2.6±0.6

Values are shown as the mean ± the standard deviation. Each group comprised 12 implants in bilateral knee joints from 6 animals (2 each). The letters *a*, *b*, *c* and *d* indicate a significant difference from the MSC/MSC, MSC/OS, CG7/OS and CS14/OS groups, respectively.

Table 3

Mean histological scores for cell-laden hydrogel formulations at randomly chosen peripheral edges (medial or lateral) of the defects 12 weeks postsurgery.

Histological Parameter	Left Knee Scores (24 knees total)				Right Knee Scores (24 knees total)			
	MSC/MSC (6 knees)	MSC/OS (6 knees)	CG7/OS (6 knees)	CG14/OS (6 knees)	MSC/MSC (6 knees)	MSC/OS (6 knees)	CG7/OS (6 knees)	CG14/OS (6 knees)
Overall evaluation								
1.	2.2±0.4	2.5±0.6	2.2±0.4	2.0±0.0	2.0±0.0	2.2±0.4	2.3±0.5	2.2±0.4
2.	2.3±0.5	2.5±0.6	2.2±0.4	2.0±0.0	2.2±0.4	2.2±0.4	2.3±0.5	2.2±0.4
Bone evaluation								
3.	2.2±0.8	2.5±0.6	2.0±0.6	2.0±0.0	2.2±0.4	2.0±0.6	2.2±0.8	2.0±0.6
4.	1.7±1.0	1.8±1.3	1.3±0.8	1.0±0.0	0.8±0.4	1.5±1.2	2.0±1.6	1.0±0.0
5.	3.0±0.0	3.0±0.0	3.0±0.0	3.0±0.0	3.0±0.0	3.0±0.0	3.0±0.0	3.0±0.0
Cartilage evaluation								
6.	2.5±0.6	2.7±0.8	2.7±0.5	2.3±0.5	2.0±0.6	2.8±0.6[d]	3.0±0.9[d]	2.0±0.0[b,c]
7.	1.3±0.5[b]	2.2±0.4[a]	1.8±0.8	1.8±0.8	1.5±0.6[b]	2.7±0.8[a]	2.2±1.0	1.8±0.8
8.	2.2±0.8[b]	3.0±0.0[a,c]	1.8±0.8[b]	1.8±1.5	1.7±0.8	2.3±0.5	2.5±0.6	2.5±0.6
9.	2.2±0.8	2.0±0.0	1.8±0.4	2.5±0.6	2.0±0.6	2.0±0.6	2.5±0.6	2.3±0.5
10.	1.7±0.8	1.8±0.8	2.0±0.6	1.8±0.8	1.7±0.8	1.8±0.8	2.0±0.9	1.5±0.6
11.	2.8±0.4	2.8±0.4	2.8±0.4	2.8±0.4	2.8±0.4	2.7±0.5	2.7±0.5	2.7±0.5

Values are shown as the mean ± the standard deviation. Comparisons were made between groups for the same knee, where each group comprised 6 unilateral implants from 6 animals. The letters *a*, *b*, *c* and *d* indicate a significant difference from the MSC/MSC, MSC/OS, CG7/OS and CG14/OS groups, respectively.